 CMES, vol.80, no.2, pp.113-140, 2011

Probabilistic Analysis of Transient Problems by the Least Squares Stochastic Perturbation-Based Finite Element Method

M.M. Kaminski[1]

Abstract: The main aim of this work is to demonstrate a solution to the transient problems for the statistically homogeneous media with random physical parameters. This is done with the use of the stochastic perturbation technique based on the general order Taylor series expansions and the additionally modified implementation of the Finite Element Method. Now, both the Direct Differentiation Method as well as the Response Function Method are employed to form and solve up to the *n*th order state equations. Computational implementation of both approaches is illustrated using two examples – by determination of the probabilistic moments of the temperature histories in the heated rod with the constant prismatic cross-section as well as for the two degrees of freedom elastic system subjected to the forced vibrations. The proposed numerical technique may also find an application in the transient heat transfer or elastodynamics in the large scale structures, for both homogeneous and heterogeneous media modelling, where physical parameters may be defined as the stochastic processes like time series, for instance.

Keywords: response function method, transient heat transfer, forced vibrations, modal superposition method, Finite Element Method.

1 Introduction

Efficient numerical solution of the transient problems with random parameters plays the very important role in modern engineering, because such problems are closely related to many modern applications and still are a subject of many works [Hurtado (2002), Papadopoulos and Papadrakakis (2006), Spanos (2005), Schueller (2007)]. The second need is optimal modelling, considering computational time, power and efficiency, of non-Gaussian random variables, fields and processes, where

[1] Department of Steel Structures, Faculty of Civil Engrg., Arch. & Env. Engrg., Technical University of Lodz, 90-924 Lodz, Al. Politechniki 6, Poland, Marcin.Kaminski@p.lodz.pl

the first two probabilistic moments do not give a complete information about the resulting uncertainty and should be accompanied with higher order statistics. It follows mainly the need of engineering reliability analysis, which in case of transient analyses may be sometimes time-dependent problem. On the other hand, a successful application of the Monte-Carlo simulation (in any of the versions and computers available) depends on the fact, whether we are able to predict in some way the expected type of the output statistical behaviour (remarkable time savings) or not, but computational effort may be anyway tremendous. The non-statistical methods have difficulties with determination of higher than the second order statistics but with their significant time savings it is still worth to explore their details to find such opportunities - the Second Order Second Moment application of the stochastic perturbation technique to the solution of the linear transient heat transfer can be found in [Hien and Kleiber (1997)].

The main aim of this work is just dedicated to such an alternative method, where the generalized stochastic perturbation method (GSPM) is used in a dual formulation to solve some illustrative transient problems with random parameters. Although initially we use Gaussian design parameters but other probability density functions are also admissible in this formulation, whereas a duality means that the higher order partial derivatives of the structural response, as the immanent part of GSPM, may be determined using the Direct Differentiation Method [Belytschko et al (1986), Kleiber and Hien (1992)] or – with the use of the Response Function Method [Kaminski (2010)]. This second method is somewhat similar to the Response Surface Method explored widely in the stochastic reliability area [Khuri and Cornell (1986)], but a major difference is a presence of higher order polynomials (up to the given order) and, mainly, the opportunity to use both global and local formulations applied before in sensitivity analysis [Kaminski (2011)]. Concerning some previous implementations, now the RFM technique is presented in its weighted least square approach enabling for polynomial interrelation (some specific forms are also available from analytical solutions – see [Elishakoff (1995)] in-between output and input parameters for the given nodal point of the mesh; the mesh size is not an important issue [Kaminski (2011)]. The final probabilistic structural response, analyzed here for the temperature and displacements histories, is given in the form of the first four probabilistic moments of those responses given as a function of the input coefficient of variation. Transient heat transfer example is solved using the RFM-SFEM strategy, while th transient dynamic analysis has been provided by the straightforward DDM-SFEM approach. The main difference in-between those two computational implementations of the SFEM concerning possible numerical errors is – solution of higher order equilibrium equations in case of the DDM and RFM – determination of the higher order partial derivatives on the base of the least squares

technique approximation. A comparison against the crude Monte-Carlo simulation has been studied in [Kaminski (2010)], while the computational effort of the technique proposed is comparable to the deterministic solution except a necessity of the computer algebra software programming and common usage with the FEM core. The results may find wide application in the reliability-oriented optimization of engineering structures and systems with random parameters or vibrations [Van Noortwijk (2004)], also in terms of composite materials application and including the stochastic ageing processes of some components.

2 Governing equations

2.1 Transient heat transfer analysis

Generally, transient heat flow problem consists in determining the temperature field T=$T(\mathbf{x},\tau)$ governed by the following differential equation [Carlsaw and Jaeger (1959)]:

$$\rho\, c\dot{T} - \left(\lambda_{ij}T_{,j}\right)_{,i} - g = 0; \quad x_i \in \Omega;\ \tau \in [0,\infty), \tag{1}$$

where c is the heat capacity characterizing the region Ω, ρ is the density of the material contained in Ω, λ_{ij} is the thermal conductivity second order tensor, while g is the rate of heat generated per unit volume; the variables T and τ denote temperature field values and time, respectively. This equation should fulfil the boundary conditions of the $\partial\Omega$, which are given as follows:

1) temperature (essential) boundary conditions

$$T = \hat{T}; \quad x \in \partial\Omega_T, \tag{2}$$

and for $\partial\Omega_q$ part of the total $\partial\Omega$:

2) heat flux (natural) boundary conditions

$$\frac{\partial T}{\partial n} = \hat{q}; \quad x \in \partial\Omega_q, \tag{3}$$

where $\partial\Omega_T \cup \partial\Omega_q = \partial\Omega$ and also $\partial\Omega_T \cap \partial\Omega_q = \{\emptyset\}$.

The initial conditions are proposed here as

$$T^0 = T\left(x_i;0\right); \quad x_i \in \Omega, \quad \tau = 0. \tag{4}$$

Let us consider further some continuous temperature variations $\delta T\left(x_i\right)$ defined in the interior of the region Ω and vanishing on $\partial\Omega_T$. Multiplying Eq. (1) by the test

function and integrating over the entire Ω, we obtain

$$\int_{\Omega} \left(\rho c \dot{T} - \left(\lambda_{ij} T_{,j} \right)_{,i} - g \right) \ \delta T \ d\Omega = 0; \quad x_i \in \Omega; \quad \tau \in [0, \infty). \tag{5}$$

Taking into account that

$$\frac{\partial \left(\delta T \right)}{\partial x_i} = \delta \left(\frac{\partial T}{\partial x_i} \right) \equiv \delta T_{,i}, \tag{6}$$

and with the additional heat transfer boundary conditions we can arrive at

$$\int_{\Omega} \left(\lambda_{ij} T_{,j} \ \delta T \right)_{,i} d\Omega = \int_{\partial \Omega} \lambda_{ij} \ T_{,j} \ n_{,i} \ \delta T \ d(\delta \Omega) = \int_{\partial \Omega_q} \hat{q} \ \delta T \ d(\partial \Omega) \tag{7}$$

Then, an integration by parts gives here

$$\int_{\Omega} \left(\rho c \dot{T} \delta T + \lambda_{ij} T_{,j} \delta T_{,i} - g \delta T \right) \ d\Omega - \int_{\partial \Omega_q} \hat{q} \ \delta T \ d \left(\partial \Omega \right) = 0; \quad x_i \in \Omega; \ \tau \in [0, \infty). \tag{8}$$

The stochastic variational principle for linear transient heat transfer problems is formulated on the basis of this equation using the following expansion of the temperatures:

$$T \left(\omega \right) = T^0 \left(\omega \right) + \varepsilon \frac{\partial T \left(\omega \right)}{\partial b} \Delta b + ... + \frac{1}{n!} \varepsilon^n \frac{\partial^n T \left(\omega \right)}{\partial b^n} \Delta b^n, \tag{9}$$

where ε is a given small perturbation (taken usually as equal to 1), and where the nth order variation is given as follows:

$$\varepsilon^n \Delta b^n = \left(\delta b \right)^n = \varepsilon^n \left(b - b^0 \right)^n. \tag{10}$$

This expansion substituted into the formulation (8) results in the set of the algebraic equations of the systematically increasing order (from 0^{th} up to the nth) obtained for the consecutive powers of the perturbation parameter. There holds

zeroth-order partial differential equation

$$\int_{\Omega} \left(\rho^0 c^0 \dot{T^0} \delta T + \lambda_{ij}^0 T_{,j}^0 \delta T_{,i} \right) d\Omega = \int_{\partial \Omega_q} \hat{q}^0 \ \delta T \ d \left(\partial \Omega \right) + \int_{\Omega} g^0 \delta T \ d\Omega, \tag{11}$$

first-order partial differential equation

$$\int_{\Omega}\left(\rho^0 c^0 fr\delta\frac{\partial T}{\partial b}\delta T+\lambda_i^0\frac{\partial T_{,j}}{\partial b}\delta T_{,i}\right)d\Omega \;=\; \int_{\partial\Omega_q}\frac{\partial\hat{q}}{\partial b}\delta T\,d(\partial\Omega)+\int_{\Omega}\frac{\partial g}{\partial b}\delta T\,d\Omega$$
$$-\int_{\Omega}\left(\left(\frac{\partial\rho}{\partial b}c^0+\rho^0\frac{\partial c}{\partial b}\right)\dot{T^0}\,\delta T+\frac{\partial\lambda_{ij}}{\partial b}T^0_{,j}\delta T_{,i}\right)d\Omega, \tag{12}$$

second-order partial differential equation

$$\int_{\Omega}\left(\rho^0 c^0\frac{\partial^2\dot{T}}{\partial b^2}\,\delta T+\lambda^0_{ij}\frac{\partial^2 T_{,j}}{\partial b^2}\delta T_{,i}\right)d\Omega \;=\; \int_{\partial\Omega_q}\frac{\partial^2 q}{\partial b^2}\,\delta T\,d(\partial\Omega)+\int_{\Omega}\frac{\partial^2 g}{\partial b^2}\delta T\,d\Omega+$$
$$-\int_{\Omega}\left(\left(\frac{\partial^2\rho}{\partial b^2}c^0+2\frac{\partial\rho}{\partial b}\frac{\partial c}{\partial b}+\rho^0\frac{\partial^2 c}{\partial b^2}\right)\dot{T^0}+\left(\frac{\partial\rho}{\partial b}c^0+\rho^0\frac{\partial c}{\partial b}\right)\frac{\partial\dot{T}}{\partial b}\right)\delta T d\Omega+$$
$$-\int_{\Omega}\left(\frac{\partial^2\lambda_{ij}}{\partial b^2}T^0_{,j}+2\frac{\partial\lambda_{ij}}{\partial b}\frac{\partial T_{,j}}{\partial b}\right)\delta T_{,i}d\Omega, \tag{13}$$

as well as the nth order equation

$$\int_{\Omega}\left(\sum_{k=0}^{n}\binom{n}{k}\left(\sum_{m=0}^{k}\binom{k}{m}\frac{\partial^k\rho}{\partial b^k}\frac{\partial^{k-m}c}{\partial b^{k-m}}\right)\frac{\partial^{n-k}\dot{T}}{\partial b^{n-k}}\right)\delta T d\Omega$$
$$+\int_{\Omega}\left(\sum_{k=0}^{n}\binom{n}{k}\frac{\partial^k\lambda_{ij}}{\partial b^k}\frac{\partial^{n-k}T_{,j}}{\partial b^{n-k}}\right)\delta T_{,i}d\Omega \tag{14}$$
$$=\int_{\partial\Omega_q}\frac{\partial^n\hat{q}}{\partial b^n}\,\delta T\,d(\partial\Omega)+\int_{\Omega}\frac{\partial^n g}{\partial b^n}\delta T d\Omega$$

since most frequently those equations are solved with the randomized material parameters, we can ignore the partial derivatives of both q and g as well as higher than the first order partial derivatives of physical parameters. Having solved these equations for T^0, $\frac{\partial T}{\partial b}$ until $\frac{\partial^n T}{\partial b^n}$ respectively, we derive the expressions for the expected values and higher probabilistic moments and the coefficients for temperature field

and its histories. One may derive that the expected values are equal to

$$\begin{aligned} E\left[T\left(t\right)\right] =& T^{0}\left(t,b^{0}\right)+\frac{1}{2}\varepsilon^{2}\frac{\partial^{2}\left(T\left(t\right)\right)}{\partial b^{2}}\mu_{2}\left(b\right)+\frac{1}{4!}\varepsilon^{4}\frac{\partial^{4}\left(T\left(t\right)\right)}{\partial b^{4}}\mu_{4}\left(b\right) \\ &+\frac{1}{6!}\varepsilon^{6}\frac{\partial^{6}\left(T\left(t\right)\right)}{\partial b^{6}}\mu_{6}\left(b\right)+...+\frac{1}{(2m)!}\varepsilon^{2m}\frac{\partial^{2m}\left(T\left(t\right)\right)}{\partial b^{2m}}\mu_{2m}\left(b\right) \end{aligned} \tag{15}$$

for any natural m with μ_{2m} being the central probabilistic moment of $2m^{th}$ order. Usually, according to some previous convergence studies we may limit this expansion-type approximation to the 10^{th} order. Quite a similar considerations lead to the expressions for higher moments, like the variance, for instance,

$$\begin{aligned} &Var\left(T\left(t\right)\right)=\int_{-\infty}^{+\infty}\left(T^{0}\left(t\right)+\varepsilon\Delta b\frac{\partial T\left(t\right)}{\partial b}+\frac{1}{2}\varepsilon^{2}\left(\Delta b\right)^{2}\frac{\partial^{2}T\left(t\right)}{\partial b^{2}}+...-E\left[T\left(t\right)\right]\right)^{2}p\left(b\right)db \\ &=\varepsilon^{2}\mu_{2}\left(b\right)\left(\frac{\partial T\left(t\right)}{\partial b}\right)^{2}+\varepsilon^{4}\mu_{4}\left(b\right)\left(\frac{1}{4}\left(\frac{\partial^{2}T\left(t\right)}{\partial b^{2}}\right)^{2}+\frac{2}{3!}\frac{\partial T\left(t\right)}{\partial b}\frac{\partial T^{3}\left(t\right)}{\partial b^{3}}\right) \\ &+\varepsilon^{6}\mu_{6}\left(b\right)\left(\left(\frac{1}{3!}\right)^{2}\left(\frac{\partial T^{3}\left(t\right)}{\partial b^{3}}\right)^{2}+\frac{1}{4!}\frac{\partial^{4}T\left(t\right)}{\partial b^{4}}\frac{\partial^{2}T\left(t\right)}{\partial b^{2}}+\frac{2}{5!}\frac{\partial^{5}T\left(t\right)}{\partial b^{5}}\frac{\partial T\left(t\right)}{\partial b}\right) \end{aligned} \tag{16}$$

The central third probabilistic moment may be recovered from this scheme as

$$\begin{aligned} &\mu_{3}\left(T\left(t,b\right)\right)=\int_{-\infty}^{+\infty}\left(T\left(t,b\right)-E\left[T\left(t,b\right)\right]\right)^{3}p\left(b\right)db= \\ &=\int_{-\infty}^{+\infty}\left(\varepsilon\frac{\partial T\left(t\right)}{\partial b}\Delta b+\tfrac{1}{2}\varepsilon^{2}\tfrac{\partial^{2}T\left(t\right)}{\partial b^{2}}\Delta b\Delta b+...\right)^{3}p\left(b\right)db \\ &\cong\frac{3}{2}\varepsilon^{4}\mu_{4}\left(b\right)\left(\frac{\partial T\left(t\right)}{\partial b}\right)^{2}\frac{\partial^{2}T\left(t\right)}{\partial b^{2}}+\frac{1}{8}\varepsilon^{6}\mu_{6}\left(b\right)\left(\frac{\partial^{2}T\left(t\right)}{\partial b^{2}}\right)^{3} \end{aligned} \tag{17}$$

using the lowest order approximation. The fourth central probabilistic moment computation proceeds from the following formula:

$$\begin{aligned} &\mu_{4}\left(T\left(t,b\right)\right)=\int_{-\infty}^{+\infty}\left(T\left(t,b\right)-E\left[T\left(t,b\right)\right]\right)^{4}p\left(b\right)db \\ &\cong\varepsilon^{4}\mu_{4}\left(b\right)\left(\frac{\partial T\left(t\right)}{\partial b}\right)^{4}+\frac{3}{2}\varepsilon^{6}\mu_{6}\left(b\right)\left(\frac{\partial T\left(t\right)}{\partial b}\frac{\partial^{2}T\left(t\right)}{\partial b^{2}}\right)^{2}+\frac{1}{16}\varepsilon^{8}\mu_{8}\left(b\right)\left(\frac{\partial^{2}T\left(t\right)}{\partial b^{2}}\right)^{4} \end{aligned}$$

(18)

Determination of the coefficients of variation, skewness and kurtosis proceeds in a traditional way, directly from the corresponding definitions. As one may supposed, the higher order moments we need to compute, the higher order perturbations need to be included into those formulas, so that the complexity of computational model grows non-proportionally together with the precision and the size of the output information needed.

2.2 Variational statements for the elastodynamics

Let us consider the system of equations representing the elastodynamic problem with deterministic parameters assuming that all state variables are sufficiently smooth and continuous functions of x and τ. It consists of

(1) equations of motion

$$D_{jk}\sigma_k + \hat{f}_j = \rho\ddot{u}_j,\ \mathbf{x}\in\Omega,\ \tau\in[t_0,\infty),\ j,k=1,2,3 \tag{19}$$

(2) constitutive equations

$$\sigma_k = C_{kj}\varepsilon_j,\ \mathbf{x}\in\Omega,\ \tau\in[t_0,\infty),\ j,k=1,2,3 \tag{20}$$

(3) geometrical equations

$$\varepsilon_k = D_{kj}u_j,\ \mathbf{x}\in\Omega,\ \tau\in[t_0,\infty),\ j,k=1,2,3 \tag{21}$$

(4) displacement boundary conditions

$$u_j = \hat{\tilde{u}}_j,\ \mathbf{x}\in\partial\Omega_u,\ \tau\in[t_0,\infty), \tag{22}$$

(5) stress boundary conditions

$$N_{jk}\sigma_k = \tilde{\hat{f}}_j,\ \mathbf{x}\in\partial\Omega_u,\ \tau\in[t_0,\infty), \tag{23}$$

(6) initial conditions

$$u_j = \hat{u}_j^0,\ \dot{u}_j = \hat{\dot{u}}_j^0,\ \mathbf{x}\in\Omega_u,\ \tau=t_0. \tag{24}$$

Introducing a variation $\delta u(\mathbf{x},t)$ for any moment $\tau = t$ we obtain after integration the above equations as

$$-\int_{\Omega}\left(D_{jk}\sigma_k + \hat{f}_j - \rho\ddot{u}_j\right)^{\mathbf{T}}\delta u d\Omega + \int_{\partial\Omega_\sigma}\left(N_{jk}\sigma_k - \hat{t}_j\right)^T\delta u d(\partial\Omega) = 0 \tag{25}$$

Assuming known $u\left(\mathbf{x},t_{(p)}\right)=0$ and $u\left(\mathbf{x},t_{(k)}\right)=0$ it yields

$$\delta u\left(\mathbf{x},t_{(p)}\right)=0, \quad \delta u\left(\mathbf{x},t_{(k)}\right)=0. \tag{26}$$

Integration by parts with respect to $\mathbf{x}$ and τ gives

$$\int_{t_{(p)}}^{t_{(k)}}\left[\delta T-\int_{\Omega}\sigma_k^T\delta\varepsilon d\Omega+\int_{\Omega}\hat{f}_j^T\delta u d\Omega+\int_{\partial\Omega}\tilde{\hat{t}}_j^T\delta u d\left(\partial\Omega\right)\right]d\tau=0, \tag{27}$$

which is used together with

$$\delta\boldsymbol{\varepsilon}=D_{jk}\delta\mathbf{u}, \quad \mathbf{x}\in\Omega, \quad \tau\in[t_0,\infty),\ \delta\mathbf{u}=0, \quad \mathbf{x}\in\Omega_u, \quad \tau\in[t_0,\infty). \tag{28}$$

Providing an independence of the vectors $\hat{f}_j$ and $\hat{t}_j$ from $\mathbf{u}$, we may write

$$\delta\int_{t_{(p)}}^{t_{(k)}}\left(T-J_p\right)d\tau=0, \tag{29}$$

where

$$\begin{aligned} T&=\frac{1}{2}\int_{\Omega}\rho\dot{u}_j^T\dot{u}_j d\Omega,\\ J_p&=U-\int_{\Omega}\hat{f}_j^T u_j d\Omega-\int_{\partial\Omega_\sigma}\tilde{\hat{t}}_j^T u_j d\left(\partial\Omega\right)=0,\\ U&=\frac{1}{2}\int_{\Omega}C_{ij}\varepsilon_i\varepsilon_j d\Omega. \end{aligned} \tag{30}$$

are the kinetic and potential energies stored in the volume Ω. Determination of the basic probabilistic characteristics of the displacements, velocities and accelerations is provided similarly to Eqs. (15 - 18).

3 Computational implementation

3.1 Transient heat transfer discretization

Let us assume that the domain Ω is completely discretized using the set of finite elements and that the scalar temperature field T in Ω is described by the nodal temperatures vector θ_α [Pepper and Heinrich (1992), Krishnamoorthy (1994)]

$$T\left(x_i\right)=H_\alpha\left(x_i\right)\ \theta_\alpha;\ i=1,2;\ \alpha=1,2,\ldots,N, \tag{31}$$

where N is the total number of degrees of freedom introduced. The temperature derivatives can be written in the form

$$T_{,i} = H_{\alpha,i}\,\theta_\alpha,\ i = 1,2. \tag{32}$$

Moreover, let us introduce the heat capacity matrix $C_{\alpha\beta}$, the heat conductivity matrix $K_{\alpha\beta}$ and the vector P_α as follows:

$$\begin{aligned} C_{\alpha\beta} &= \int_\Omega \rho c\, H_\alpha\, H_\beta\, d\Omega, \\ K_{\alpha\beta} &= \int_\Omega \lambda_{ij}\, H_{\alpha,i}\, H_{\beta,j}\, d\Omega, \\ P_\alpha &= \int_\Omega g\, H_\alpha d\Omega + \int_{\partial\Omega} \hat{q}\, H_\alpha d\Omega \end{aligned} \tag{33}$$

Inserting these matrices into the variational formulation (8) we obtain the following algebraic equations system:

$$C_{\alpha\beta}\dot{\theta}_\beta + K_{\alpha\beta}\theta_\beta = P_\alpha. \tag{34}$$

The main issue in transient problems is the additional time discretization using some time increment Δt. We can rewrite the last equation in the following manner:

$$C_{\alpha\beta}\frac{\theta_\beta(t+\Delta t) - \theta_\beta(t)}{\Delta t} + K_{\alpha\beta}\theta_\beta(t) = P_\alpha. \tag{35}$$

Considering the second component in this statement we obtain the explicit method, where the nodal temperatures vector is taken at the beginning of this time step. However, it is possible to introduce the extra coefficient $0 \le \delta \le 1$ to include in this term the temperatures vector after the time step also. There holds

$$C_{\alpha\beta}\frac{\theta_\beta(t+\Delta t) - \theta_\beta(t)}{\Delta t} + K_{\alpha\beta}\left\{\delta\theta_\beta(t+\Delta t) + (1-\delta)\,\theta_\beta(t)\right\} = P_\alpha, \tag{36}$$

where δ=0 is equivalent to the explicit method, δ=1/2 serves for the Crank-Nicholson method, δ=2/3 stands for the Galerkin method and at last δ=1 is used in the implicit method (one can use this algorithm with δ as the extra input parameter); there are also three level schemes, where the temperatures in the moments $t+\Delta t$, t, $t-\Delta t$ are included at once. Further procedure leads to such a reformulation of this equation to obtain the nodal temperatures for $t+\Delta t$ at the L.H.S. and the temperatures vector

in the previous time step at the R.H.S, so that for the Crank-Nicholson scheme we proceed as follows

$$C_{\alpha\beta}\left\{\frac{\theta_\beta(t+\Delta t)-\theta_\beta(t)}{\Delta t}\right\}+K_{\alpha\beta}\left\{\frac{\theta_\beta(t+\Delta t)}{2}+\frac{\theta_\beta(t)}{2}\right\}=P_\alpha, \tag{37}$$

therefore

$$\left(\frac{C_{\alpha\beta}}{\Delta t}+\frac{K_{\alpha\beta}}{2}\right)\theta_\beta(t+\Delta t)=P_\alpha+\left(\frac{C_{\alpha\beta}}{\Delta t}-\frac{K_{\alpha\beta}}{2}\right)\theta_\beta(t). \tag{38}$$

An introduction of the matrix $D_{\alpha\beta}$ instead of a combination of the heat conductivity and heat capacity matrices at the L.H.S. as well as the additional matrix $E_{\alpha\beta}$ for the R.H.S. bracket leads to the relation:

$$D_{\alpha\beta}\theta_\beta(t+\Delta t)=P_\alpha+E_{\alpha\beta}\theta_\beta(t). \tag{39}$$

Analogously to the previous considerations we can obtain the following systems of algebraic equations describing the second- or higher-order stochastic formulation of the transient heat flow problem:

zeroth-order equation

$$C^0_{\alpha\beta}\dot\theta^0_\beta+K^0_{\alpha\beta}\theta^0_\beta=P^0_\alpha, \tag{40}$$

first-order equation

$$C^0_{\alpha\beta}\frac{\partial\dot\theta_\beta}{\partial b}+K^0_{\alpha\beta}\frac{\partial\theta_\beta}{\partial b}=\frac{\partial P_\alpha}{\partial b}-\left(\frac{\partial C_{\alpha\beta}}{\partial b}\dot\theta^0_\beta+\frac{\partial K_{\alpha\beta}}{\partial b}\theta^0_\beta\right), \tag{41}$$

second-order equation

$$\begin{aligned}&C^0_{\alpha\beta}\frac{\partial^2\dot\theta_\beta}{\partial b^2}+K^0_{\alpha\beta}\frac{\partial^2\theta_\beta}{\partial b^2}=\\&\frac{\partial^2P_\alpha}{\partial b^2}-2\left(\frac{\partial C_{\alpha\beta}}{\partial b}\frac{\partial\dot\theta_\beta}{\partial b}+\frac{\partial K_{\alpha\beta}}{\partial b}\frac{\partial\theta_\beta}{\partial b}\right)-\left(\frac{\partial^2C_{\alpha\beta}}{\partial b^2}\dot\theta^0_\beta+\frac{\partial^2K_{\alpha\beta}}{\partial b^2}\theta^0_\beta\right)\end{aligned} \tag{42}$$

and, at last, the nth order equation

$$\begin{aligned}&C^0_{\alpha\beta}\frac{\partial^n\dot\theta_\beta}{\partial b^n}+K^0_{\alpha\beta}\frac{\partial^n\theta_\beta}{\partial b^n}=\\&\frac{\partial^nP_\alpha}{\partial b^n}-\sum_{k=1}^{n}\binom{n}{k}\frac{\partial^kC_{\alpha\beta}}{\partial b^k}\frac{\partial^{n-k}\dot\theta_\beta}{\partial b^{n-k}}-\sum_{k=1}^{n}\binom{n}{k}\frac{\partial^kK_{\alpha\beta}}{\partial b^k}\frac{\partial^{n-k}\theta_\beta}{\partial b^{n-k}},\end{aligned} \tag{43}$$

In the equations stated above we have introduced the following matrix notation: the heat capacity matrix and its derivatives

$$C^0_{\alpha\beta} = \int_\Omega \rho^0 c^0 H_\alpha H_\beta d\Omega, \quad \frac{\partial^n C_{\alpha\beta}}{\partial b^n} = \int_\Omega \sum_{k=0}^{n} \binom{n}{k} \frac{\partial^k \rho}{\partial b^k} \frac{\partial^{n-k} c}{\partial b^{n-k}} H_\alpha H_\beta d\Omega \tag{44}$$

the heat conductivity matrix and its derivatives

$$K^0_{\alpha\beta} = \int_\Omega \lambda^0_{ij} H_{\alpha,i} H_{\beta,j} d\Omega, \quad \frac{\partial^n K_{\alpha\beta}}{\partial b^n} = \int_\Omega \frac{\partial^n \lambda_{ij}}{\partial b^n} H_{\alpha,i} H_{\beta,j} d\Omega \tag{45}$$

the right-hand vector and its derivatives

$$P^0_\alpha = \int_\Omega g^0 H_\alpha d\Omega + \int_{\partial\Omega_q} \hat{q}^0 H_\alpha d\Omega, \quad \frac{\partial^n P_\alpha}{\partial b^n} = \int_\Omega \frac{\partial^n g}{\partial b^n} H_\alpha d\Omega + \int_{\partial\Omega_q} \frac{\partial^n \hat{q}}{\partial b^n} H_\alpha d\Omega \tag{46}$$

where all those expressions are evaluated at the expected values of the input random variable. As it is clear now, the DDM version needs a formation and the solution of the increasing order equations obtained from the initial one by a systematic differentiation with respect to the random input variable provided in a quite deterministic way.

The main idea behind the Response Function Method is to recover the polynomial approximation of the temperature in a given node with respect to the input random variable b in the following form:

$$\theta_\beta = \Theta^{(m)}_\beta b^m, \; m = 0, \ldots, n-1; \; \beta = 1, \ldots, N. \tag{47}$$

so that there holds

$$T(x_i) = H_\beta(x_i) \;\; \theta_\beta = H_\beta(x_i) \;\; \Theta^{(m)}_\beta b^m; i = 1,2; \; \alpha = 1,2,...,N, \; m = 0, \ldots, n-1; \tag{48}$$

Therefore, the temperature gradients are similarly determined as

$$T_{,j} = H_{\beta,j} \, \theta_\beta = H_{\beta,j} \, \Theta^{(m)}_\beta b^m, \; i = 1,2, \; m = 0, \ldots, n-1. \tag{49}$$

The key feature of this approach is to determine numerically the coefficients $\Theta^{(m)}_\beta$ for each node of the initial FEM mesh and each power of the polynomial representations of the nodal temperatures with respect to the random input. We consider for

this purpose N sets of m data points $\left(b^{(i)}, T_\beta^{(i)}\right)$ for β=1,...,N, the nonlinear continuous function $T_\beta = f(b)$ and the curves (approximating functions) $T_\beta = f\left(b, \Theta_\beta\right)$ additionally depending on n parameters $\Theta_\beta^{(j)}$, j=1,...,n, where $m \geq n$. We define the additional residuals $r_i\left(T_\beta\right)$ as

$$r_{\beta(i)} = r_i\left(T_\beta\right) = T_\beta^{(i)} - f\left(b^{(i)}, \Theta_\beta^{(i)}\right) \tag{50}$$

to determine the unknown coefficients $\Theta_\beta^{(j)}$ from the minimization of the following functionals:

$$S_\beta = \sum_{i=1}^{m} w_{ii} r_{\beta(i)}^2 \quad , \beta = 1, ..., N \tag{51}$$

It proceeds using the gradient method, so that

$$\frac{\partial S_\beta}{\partial \Theta_\beta^{(j)}} = -2 \sum_{i=1}^{n} w_{ii} r_{\beta(i)} \frac{\partial f\left(b^{(i)}, \Theta_\beta^{(i)}\right)}{\partial \Theta_\beta^{(j)}} = 0; \tag{52}$$
$$j = 1, ..., n;\ \beta = 1, ..., N\ (\textit{no summation over } \beta)$$

Further, we adopt the following notation:

$$D_{ij}^\beta = \frac{\partial f\left(b^{(i)}, \Theta_\beta^{(i)}\right)}{\partial \Theta_\beta^{(j)}}; \quad j = 1, ..., n;\ \beta = 1, ..., N. \tag{53}$$

and we form the modified equations as

$$\sum_{i=1}^{n} \sum_{k=1}^{m} D_{ij}^\beta w_{ii} D_{ik}^\beta \Theta_\beta^{(k)} = \sum_{i=1}^{n} D_{ij}^\beta w_{ii} T_\beta^{(i)}, \quad j = 1, ..., n,\ \beta = 1, ..., N \tag{54}$$

taking the matrix form

$$\left(\left(\mathbf{D}^\beta\right)^T \mathbf{w}\, \mathbf{D}^\beta\right) \mathbf{\Theta}_\beta = \left(\mathbf{\Theta}_\beta\right)^T \mathbf{w}\, \mathbf{T}_\beta \tag{55}$$

After numerical solution to this equation for $\mathbf{\Theta}_\beta$, the final nodal polynomial approximations of the temperatures with respect to the given random variable are found together with, analytically, up to kth order ordinary derivatives of the nodal responses $\theta_\beta(b)$ with respect to b at the given b_0 as

$$\frac{d^k \theta_\beta}{db^k} = \prod_{i=1}^{k} (n-i)\, D_{\beta 1} b^{n-k} + \prod_{i=2}^{k} (n-i)\, D_{\beta 2} b^{n-(k+1)} + ... + D_{\beta n-k}. \tag{56}$$

This differentiation has quite analytical character and the increasing order partial derivatives of the nodal temperatures with respect to the random variable are not so much affected by the numerical errors from the hierarchical equations solutions. It is also clear that the probabilistic transient problem needs successive polynomial responses from time increment to the time increment, therefore for a discrete time moment τ Eq. (47) is reformulated in the following manner:

$$\theta_\beta(\tau) = \Theta_\beta^m \tau b^m,\ m = 0,\ldots,n-1;\ \beta = 1,\ldots,N. \tag{57}$$

Hence, it yields

$$T(x_i,\tau) = H_\beta(x_i)\ \ \theta_\beta(\tau) = H_\beta(x_i)\ \ \Theta_\beta^m \tau b^m; \\ i = 1,2;\ \alpha = 1,2,...,N,\ m = 0,\ldots,n-1; \tag{58}$$

Therefore, the temperature gradients are similarly determined as

$$T_{,j}(\tau) = H_{\beta,j}\,\theta_\beta(\tau) = H_{\beta,j}\,\Theta_\beta^m \tau b^m,\ i = 1,2,\ m = 0,\ldots,n-1. \tag{59}$$

Finally, one realizes that the temperature-dependent physical parameters (as well as application of the non-stationary stochastic processes) may lead to further numerical complications in Stochastic Finite Element Method implementation to transient problems using the Response Function Method. The numerical solution may also proceed using stochastic perturbation version of the Finite Difference Method [Collatz (1966)], when necessary.

3.2 Elastodynamics discretization via the stochastic finite elements

Let us consider the following approximation of the displacement field $\mathbf{u}(\mathbf{x},\tau)$ [Bathe (1996), Kleiber (1989)]

$$\mathbf{u}(\mathbf{x},\tau) = \boldsymbol{\varphi}(\mathbf{x})\ \mathbf{q}(\tau) = \boldsymbol{\varphi}(\mathbf{x})\ \mathbf{r}(\tau), \tag{60}$$

where $\mathbf{q}$ is the generalized coordinates vector for the given finite element and $\mathbf{r}$ – the global vector and while $\boldsymbol{\varphi}$, $\boldsymbol{\varphi}$ are the corresponding local and global shape functions matrices. The strain tensor is rewritten as

$$\boldsymbol{\varepsilon}(\mathbf{x},\tau) = \mathbf{B}_\varphi(\mathbf{x})\ \mathbf{q}(\tau) = \mathbf{B}_\varphi(\mathbf{x})\ \mathbf{r}(\tau) \tag{61}$$

Therefore, Eq. (27) is obtained in the global version using the loading vector of the system $\mathbf{R}(x,\tau)$

$$\delta \int_{t_{(p)}}^{t_{(k)}} \left[\frac{1}{2}\dot{\mathbf{r}}\,\mathbf{M}\,\dot{\mathbf{r}} - \frac{1}{2}\mathbf{r}\,\mathbf{K}\,\mathbf{r} + \mathbf{R}^T\mathbf{r}\right] d\tau = 0 \tag{62}$$

where the matrices of mass and stiffness are introduced as

$$\mathbf{M}=\int_{\Omega}\rho\left(\mathbf{x}\right)\mathbf{B}_{\varphi}^{T}\left(\mathbf{x}\right)\mathbf{B}_{\varphi}\left(\mathbf{x}\right)d\Omega\quad\mathbf{K}=\int_{\Omega}\mathbf{B}_{\varphi}^{\mathbf{T}}\left(\mathbf{x}\right)\mathbf{C}\mathbf{B}_{\varphi}\left(\mathbf{x}\right)d\Omega. \tag{63}$$

An integration with respect to time variable and variation leads to

$$\dot{\mathbf{r}}\mathbf{M}\delta\mathbf{r}-\int_{t_{(p)}}^{t_{(k)}}\left(\ddot{\mathbf{r}}\mathbf{M}+\mathbf{r}\mathbf{K}-\mathbf{R}^{T}\right)\partial\mathbf{r}\partial\tau=0 \tag{64}$$

so that, in the view of

$$\delta\mathbf{r}\left(t_{(p)}\right)=0,\quad\delta\mathbf{r}\left(t_{(k)}\right)=0, \tag{65}$$

the stationarity principle leads to the well known matrix equation of motion

$$\mathbf{M}\,\ddot{\mathbf{r}}+\mathbf{K}\,\mathbf{r}=\mathbf{R} \tag{66}$$

which is frequently proposed including the damping component as

$$\mathbf{M}\,\ddot{\mathbf{r}}+\mathbf{C}\,\dot{\mathbf{r}}+\mathbf{K}\,\mathbf{r}=\mathbf{R} \tag{67}$$

Modal analysis is based on the following transform:

$$\mathbf{r}\left(\tau\right)=\sum_{j=1}^{n}\mathbf{a}_{j}x_{j}\left(\tau\right)=\mathbf{A}\mathbf{x}\left(\tau\right), \tag{68}$$

where $\mathbf{A}=[\mathbf{a}_i]$ is composed with the structure eigenvectors, while $\mathbf{x}\left(\tau\right)$ is the vector of modal coordinates. The global equation of motion is transformed into

$$\sum_{j=1}^{n}\mathbf{a}_{i}^{T}\mathbf{M}\mathbf{a}_{j}\ddot{x}_{j}\left(\tau\right)+\sum_{j=1}^{n}\mathbf{a}_{i}^{T}\mathbf{C}\mathbf{a}_{j}\dot{x}_{j}\left(\tau\right)+\sum_{j=1}^{n}\mathbf{a}_{i}^{T}\mathbf{K}\mathbf{a}_{j}x_{j}\left(\tau\right)=\mathbf{a}_{i}^{T}\mathbf{R}\left(\tau\right), \tag{69}$$

The orthogonality condition on the eigenvectors leads to

$$\mathbf{a}_{i}^{T}\mathbf{M}\mathbf{a}_{i}=\begin{cases}0 & i\neq j\\ \tilde{m}_{i} & i=j\end{cases},\quad\mathbf{a}_{i}^{T}\mathbf{K}\mathbf{a}_{i}=\begin{cases}0 & i\neq j\\ \tilde{k}_{i} & i=j\end{cases}. \tag{70}$$

where $\tilde{m}_i,\tilde{k}_i$ stand for the modal mass and stiffness. Then

$$\sum_{j=1}^{n}\mathbf{a}_{i}^{T}\mathbf{M}\mathbf{a}_{j}\ddot{x}_{j}\left(\tau\right)=\tilde{m}_{i}\ddot{x}_{i}\left(\tau\right),\quad\sum_{j=1}^{n}\mathbf{a}_{i}^{T}\mathbf{K}\mathbf{a}_{j}x_{j}\left(\tau\right)=\tilde{k}_{i}x_{i}\left(\tau\right). \tag{71}$$

Introducing further modal loading vector and modal damping matrix in case of proportionality to mass and stiffnesses components (i.e. $\mathbf{C} = \alpha\mathbf{M} + \kappa\mathbf{K}$)

$$\tilde{p}_i(\tau) = \mathbf{a}_i^T \mathbf{R}(\tau), \quad \sum_{j=1}^{n} \mathbf{a}_i^T \mathbf{C}\mathbf{a}_j \dot{x}_j(\tau) = \tilde{c}_i \dot{x}_i(\tau). \tag{72}$$

so that the equation of motion becomes

$$\tilde{m}_i \ddot{x}_i(\tau) + \tilde{c}_i \dot{x}_i(\tau) + \tilde{k}_i x_i(\tau) = \tilde{p}_i(\tau), \; i = 1,2,3,...,n. \tag{73}$$

Normalization of the eigenvectors gives $\mathbf{a}_i^T \mathbf{M}\mathbf{a}_i = 1$ and $\tilde{m}_i = 1$, $\tilde{k}_i = \omega_i^2$, $\tilde{c}_i = 2\gamma_i\omega_i$, therefore

$$\ddot{x}_i(\tau) + 2\gamma_i\omega_i \dot{x}_i(\tau) + \omega_i^2 x_i(\tau) = \tilde{p}_i(\tau). \tag{74}$$

This transformation is also used to express the initial conditions, hence

$$\mathbf{r}(0) = \sum_{j=1}^{n} \mathbf{a}_j x_j(0), \quad \dot{\mathbf{r}}(0) = \sum_{j=1}^{n} \mathbf{a}_j \dot{x}_j(0), \tag{75}$$

and

$$\mathbf{x}(0) = \mathbf{A}^T \mathbf{M}\mathbf{q}(0), \quad \dot{\mathbf{x}}(0) = \mathbf{A}^T \mathbf{M}\mathbf{v}(0). \tag{76}$$

A complete solution of Eq. (73) is given as the Duhamel integral

$$x_i(\tau) = \{A_{i1}\cos\omega_{id}\tau + A_{i2}\sin\omega_{id}\tau\}\exp(-\gamma_i\omega_i\tau) + \int_0^t \tilde{p}_i(\tau)\, h_i(t-\tau)\, d\tau. \tag{77}$$

The elastic forces vector in the initial system may be determined as

$$\mathbf{f}_s(\tau) = \sum_{i=1}^{n} \mathbf{K}\mathbf{a}_i x_i(\tau) = \sum_{i=1}^{n} \omega_i^2 \mathbf{M}\mathbf{a}_i x_i(\tau) \tag{78}$$

Once we calculate the eigenfrequencies as a result of

$$\left(\mathbf{K} - \varpi^2\mathbf{M}\right)\boldsymbol{\varphi} = 0. \tag{79}$$

then we start from zeroth order relation

$$\left(\mathrm{K}^0 - \left(\varpi^0\right)^2 \mathbf{M}^0\right)\boldsymbol{\varphi}^0 = 0. \tag{80}$$

and after single partial differentiation w.r.t. b there holds

$$\left(\frac{\partial \mathbf{K}}{\partial b}-\left(\frac{\partial}{\partial b}\left(\varpi^{0}\right)^{2}\right)\mathbf{M}^{0}-\left(\varpi^{0}\right)^{2}\frac{\partial \mathbf{M}}{\partial b}\right)\boldsymbol{\varphi}^{0}=-\left(\mathbf{K}^{0}-\left(\varpi^{0}\right)^{2}\mathbf{M}^{0}\right)\frac{\partial \boldsymbol{\varphi}}{\partial b}. \tag{81}$$

A sequential differentiation up to the nth order leads to the following recursive form:

$$\begin{aligned}&\sum_{k=0}^{n}\binom{n}{k}\frac{\partial^{n-k}\mathbf{K}}{\partial b^{n-k}}\frac{\partial^{k}\boldsymbol{\varphi}}{\partial b^{k}}=\\&=\sum_{k=0}^{n}\binom{n}{k}\sum_{l=0}^{k-1}\binom{k-1}{l}\frac{\partial^{(k-(l+1))}(2\varpi)}{\partial b^{(k-(l+1))}}\frac{\partial^{l+1}\varpi}{\partial b^{l+1}}\sum_{m=0}^{n-k}\binom{n-k}{m}\frac{\partial^{m}\mathbf{M}}{\partial b^{m}}\frac{\partial^{(n-k-m)}\boldsymbol{\varphi}}{\partial b^{n-k-m}}\end{aligned} \tag{82}$$

Similarly one can write for the forced vibrations in the perturbation-based nth order version as

$$\sum_{k=1}^{n}\binom{n}{k}\left\{\frac{\partial^{n-k}\mathbf{M}}{\partial b^{n-k}}\frac{\partial^{k}\ddot{\mathbf{r}}}{\partial b^{k}}+\frac{\partial^{n-k}\mathbf{C}}{\partial b^{n-k}}\frac{\partial^{k}\dot{\mathbf{r}}}{\partial b^{k}}+\frac{\partial^{n-k}\mathbf{K}}{\partial b^{n-k}}\frac{\partial^{k}\mathbf{r}}{\partial b^{k}}\right\}=\frac{\partial^{n}\mathbf{R}}{\partial b^{n}} \tag{83}$$

or the modal equations system

$$\frac{\partial^{n}\ddot{x}_{i}(\tau)}{\partial b^{n}}+\sum_{k=1}^{n}\binom{n}{k}\left\{2\frac{\partial^{n-k}(\gamma_{i}\omega_{i})}{\partial b^{n-k}}\frac{\partial^{k}(\dot{x}_{i}(\tau))}{\partial b^{k}}+\frac{\partial^{n-k}\left(\omega_{i}^{2}\right)}{\partial b^{n-k}}\frac{\partial^{k}(x_{i}(\tau))}{\partial b^{k}}\right\}=\frac{\partial^{n}\tilde{p}_{i}(\tau)}{\partial b^{n}}, \tag{84}$$

where usually the right hand side vector equals 0 except zeroth order equation, since main interest is in the structural randomness; the very complex nature of Eqs. (82) and (84) follows intermediately a chain differentiation of the second powers of random state functions with respect to b. Final determination of the probabilistic moments for the elastic forces in the modal approach proceeds using differential form

$$\frac{\partial^{p}\mathbf{f}_{s}(\tau)}{\partial b^{p}}=\sum_{i=1}^{n}\frac{\partial^{p}}{\partial b^{p}}\left\{\mathbf{K}\mathbf{a}_{i}x_{i}(\tau)\right\}=\sum_{i=1}^{n}\frac{\partial^{p}}{\partial b^{p}}\left\{\omega_{i}^{2}\mathbf{M}\mathbf{a}_{i}x_{i}(\tau)\right\}. \tag{85}$$

4 Numerical illustrations

4.1 Heat transfer in statistically homogeneous slab

The first illustration is the transient heat transfer study by SFEM for the statistically homogeneous and isotropic rod with the constant cross-sectional area and

length L=2.0, where the time increment was used as Δt=2 seconds. Now sequentially the heat conductivity and heat capacity are taken as the input Gaussian random variables with $\alpha(\lambda) = 0.15 = \alpha(c)$; their expected values equal to E[λ]=0.10 and E[c]=1.0. The temperature is fixed at the left edge as T=0, the heat flux is applied at the right corner, whereas the entire structure is divided into 10 3-noded parabolic finite elements. Larger part of the computational experiment is conducted in the symbolic platform of MAPLE, v. 11, where the local response function for the additional time increments are determined and further combined into the output probabilistic moments together with the additional visualization presented below; the deterministic solution to this problem has been provided externally by the academic FEM code. The 11 point discretization in the random space is used to define the numerical probing process around the expected value of the random heat conductivity and also capacity (basic increment is adequate to 10% of this parameter expectation) and the 10^{th} order stochastic perturbation method is applied, the correctness of which was computationally studied before. The results contained in Figs. 1-8 contrast the expected values (Figs. 1 and 2), the variances (Figs. 3 and 4) as well as third (Figs. 5 and 6) and fourth probabilistic moments (Figs. 7 and 8) along this rod computed at 5, 10, 20, 30, 40, 60, 80 and 100 seconds of two transient processes. Analysis of those pairs shows that the results are similar in the case of the expectations only – they exhibit really similar behaviour and quite close values during the entire heating process. They have some local minima or maxima at the left end of the bar, undergo zero values within the first quarter of this structure and frequently reach once more some local extrema at the opposite edge of this bar. Those expectations (and variances) are generally consistent with the similar tests performed before using the second order analysis.

The second general observation that can be made on the basis of those results is that the maximum probabilistic moments values are significantly larger in the case, where heat conductivity is randomized than for the random heat capacity (although initially they have both the same coefficient of variation). The variances of temperatures within the nodes of the mesh instantaneously increase with time to reach the maximum at the steady state, whereas the corresponding variances for the random heat capacity behave in a different way. They start from the zero initial value, then reach the maximum within the time interval from 10 to 30 seconds (rather close to 20 seconds in Fig. 3) and start to decrease till almost zero. Let us note also that the variances in Fig. 4 (random heat conductivity) exhibit some small numerical discrepancies at the end adjacent to the fixed deterministic essential boundary condition; the neighbourhood of the natural boundary conditions is completely free from these variations. Both first two probabilistic moments (or their absolute values) increase almost monotonously from the left edge of the heated structure to the

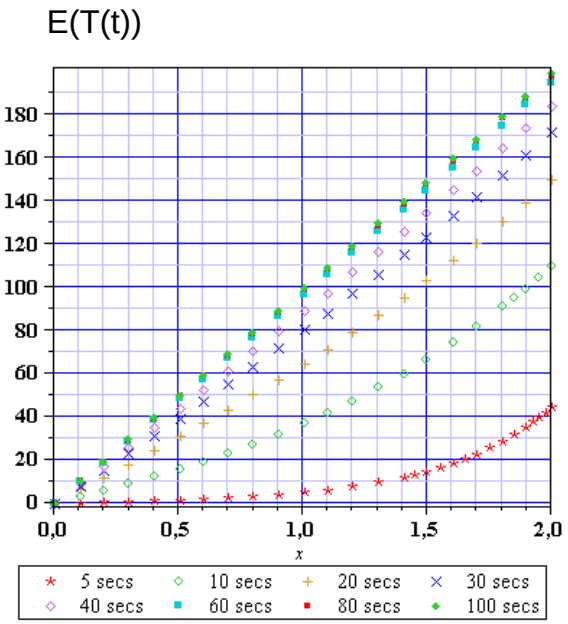

Figure 1: The expected values temperatures in the rod, random c

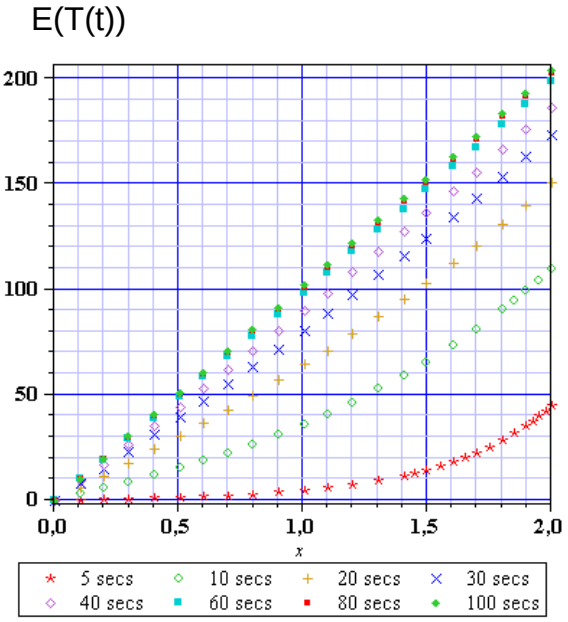

Figure 2: The expected values temperatures in the rod, random k

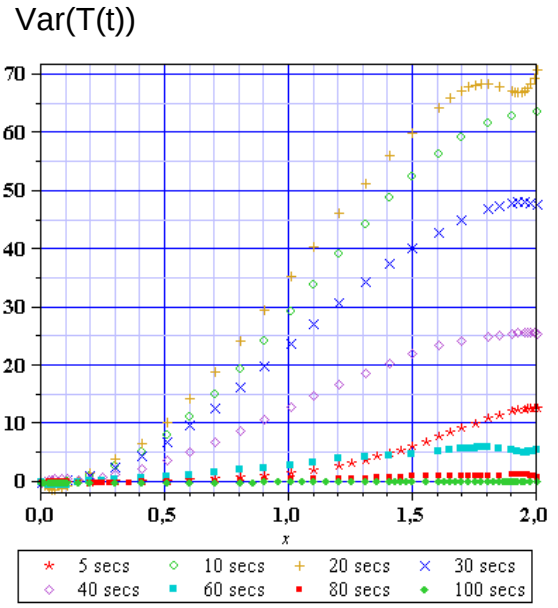

Figure 3: The variances temperatures in the rod, random c

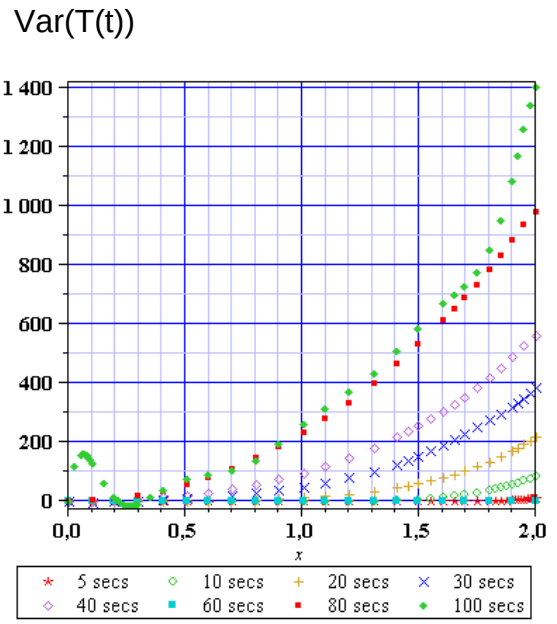

Figure 4: The variances temperatures in the rod, random k

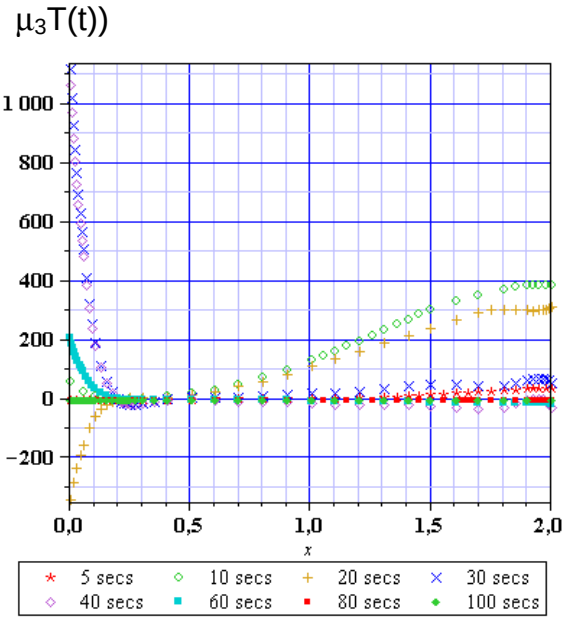

Figure 5: The 3rd probabilistic moments temperatures in the rod, random c

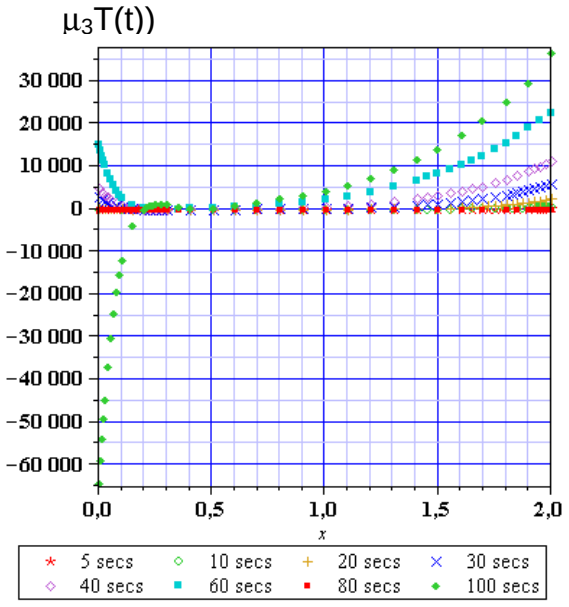

Figure 6: The 3rd probabilistic moments temperatures in the rod, random k

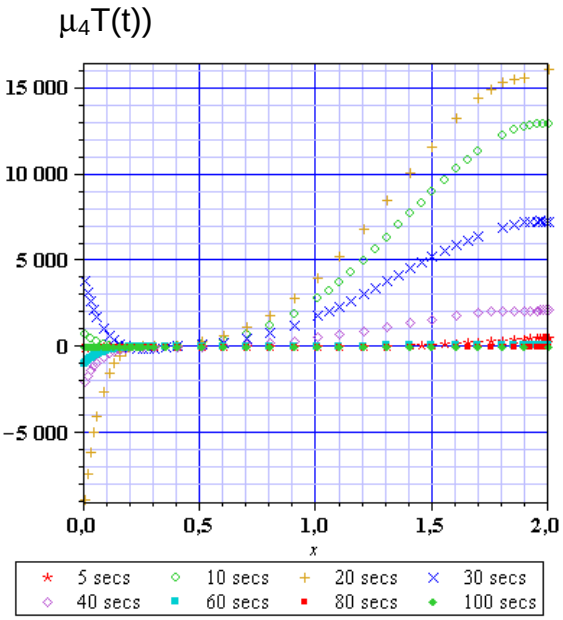

Figure 7: The 4^{th} probabilistic moments values temperatures in the rod, random c

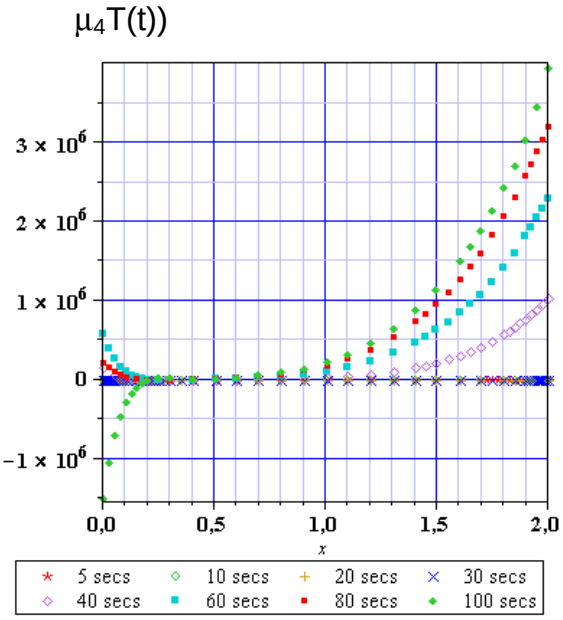

Figure 8: The 4^{th} probabilistic moments values temperatures in the rod, random k

right one, where the heat flux is applied but the higher moments apparently do not follow this rule. A comparison of the transient behaviour of those returns analogous conclusion like for the variances – randomization of the heat conductivity results in a monotonous (or almost monotonous) increase of the absolute values of those moments to the maxima at the steady state. One can notice that temperature transition with uncertain heat capacity leads to the significant growth of third and fourth probabilistic moments values (for about 20 seconds in this particular case study) and then – to nonlinear decay of those moments values at the steady state conditions. Let us note at the end that the computational cost of this analysis is relatively small – for the 11 point discretization of the random space equals to 11 times of the deterministic solution time plus relatively small amount of post-processing time to recover the nodal (time-dependent in transient analysis) response functions and to calculate the final probabilistic moments with the additional visualization. Thanks to the symbolic computations package employment one may apply easily other probability distribution as well as include the extra components to compute the cross-correlations when heat capacity and conductivity are randomized at the same time.

4.2 Modal superposition method for 2 D.O.F. system

Computational illustration for the methodology presented is illustrated with the use of the following simple case study illustrating the steel column with partially constant cross-sectional area and subjected to a certain longitudinal forced vibrations. The FEM model consists of two linear finite elements (with three nodes) and is fixed at the left end as well as loaded with the force impulse at the right hand side (Fig. 9); this load has zero magnitude in the intervals $t \in [0, t_0]$ and $t \in [t_1, \infty)$, while equals P for $t \in [t_0, t_1]$ (the deterministic counterpart of this problem is cited after Kleiber 1989). The cross sectional area A has been chosen as the truncated Gaussian input random variable with the expected value equivalent to the double HEB 1000, so that E[A]= 800 cm^2, P=1 kN, E=210 GPa, l=8.0 m, t_0=5 and t_1=5.1 secs. This choice of the random input coincides with the possible stochastic corrosion, which acting on this element may significantly decrease its effective cross-sectional area. Computational procedure based on the DDM SFEM algorithm has been entirely coded into the computer algebra system MAPLE, v. 14 to calculate up to the first four probabilistic moments and probabilistic coefficients of the displacements and elastic forces into this system (velocities and accelerations are also available).

Figures 10 and 11 presented in 3D mode show the expected values and the variances of the midpoint (node no 2) as well as the top of the column (node no 3) as the functions of time τ belonging to the short interval, when the dynamic force is at the top of the column. They are also given as the functions of the cross-sectional

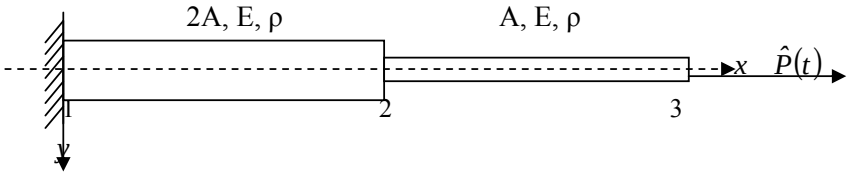

Figure 9: Computational model for the forced vibrations

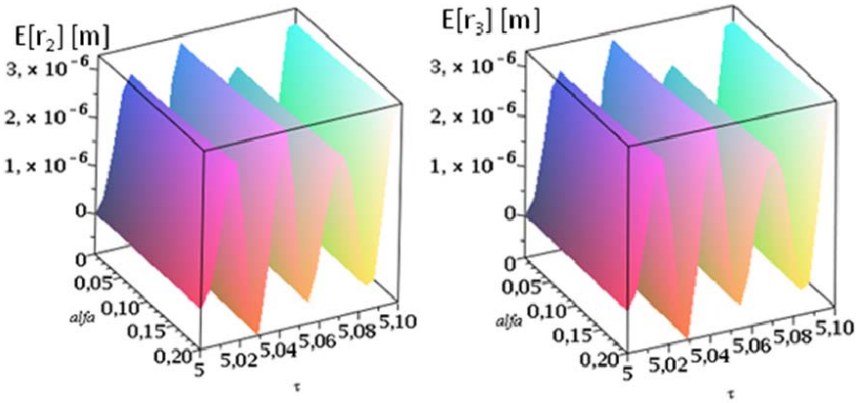

Figure 10: The expected values of the displacements in the midpoint and the top (right)

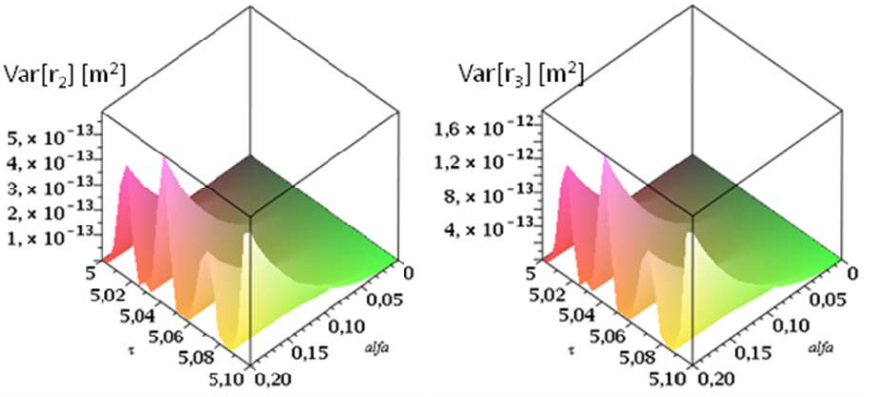

Figure 11: Variances of the displacements in the midpoint (left) and the top (right)

area coefficient of variation $\alpha \in [0.0, 0.2]$. This randomness in steel structures may correspond to the corrosion exposition, where at the initial stages of the structure exploitation this coefficient may reach in marine environments even 0.50 (then it usually stabilizes to 0.10). As one could expect, the mean values (given in [m]) are totally independent from this coefficient and vary together with time only; the absolute values have exactly the same values, while the local extrema coincide perfectly. Somewhat contrary to the expectations, the variances are highly dependent (convex nonlinearity) on the initial uncertainty having extremum values for $\alpha = 0.2$. Local extrema for the variances coincide with those computed for the expectations resulting in the maxima of coefficients of variations reaching the values close to 0.2. Finally, the variances obtained for the top of column, are about three times larger than for the midpoint in this element, so that the largest uncertainty is noticed at the top of the column where the dynamic excitation has been applied.

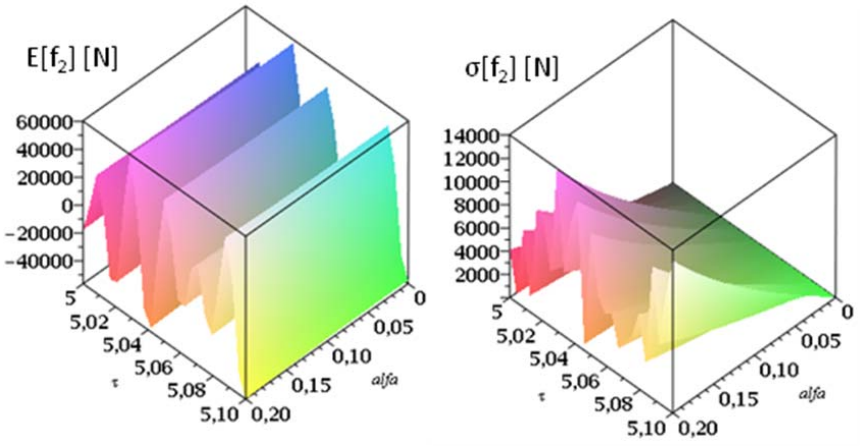

Figure 12: The expected values and standard deviation (right) of the midpoint force

Further, the expected values, standard deviations, the third and fourth central probabilistic moments of the elastic force are determined for the midpoint of the column – the probabilistic study of this force at the top (not attached here) shows clearly pure determinism in this state variable. They are shown in Figs. 12 and 13 in the same domain $f=f(\tau,\alpha)$. All the moments except expectations are significantly dependent on the initial randomness having the values increasing together with this parameter. A comparison of the left diagram in Fig. 12 with analogous in Fig. 10 shows that the elastic force has larger number of local extrema in this time period than the corresponding displacement. A dominating character of positive values of expectations remains clear after the dynamic force impulsively extending this

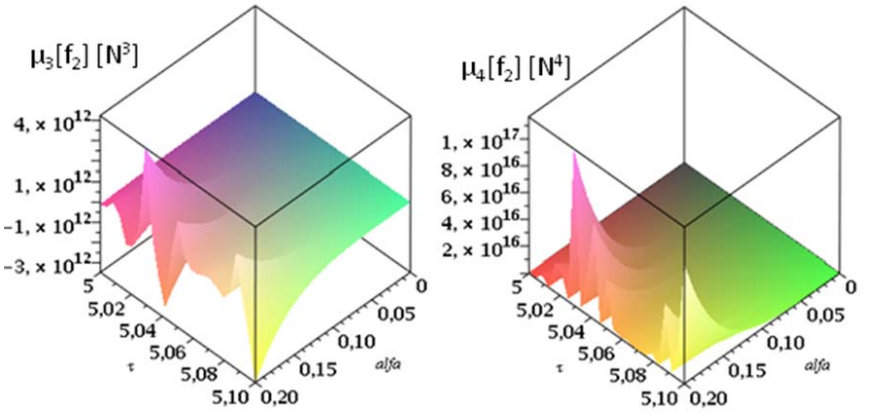

Figure 13: The third and fourth (right) probabilistic moments of the midpoint force

structure (analogously displacements in Fig. 10). Standard deviations are almost linearly dependent on the cross-sectional coefficient of variation, while third and fourth order moments – highly nonlinear. Figure 13 presents moreover that those higher moments are almost equal 0 for $\alpha \in [0.0, 0.1]$, which means that elastic forces may be treated as Gaussian variables within this interval. Of course, the higher probabilistic moment, the larger absolute extremum values within the analyzed time interval.

5 Concluding remarks

[1] As it was documented in this paper, there are two methods available of computational implementation of the generalized perturbation-based finite element method. These are the (1) Direct Differentiation Method, where the partial differentiation process is carried out analytically on the initial elemental matrices to be combined into the hierarchical equations of up to the given order and (2) the Response Function Method, where polynomial approximation between the stochastic nodal output and the random input parameter is numerically recovered. The main advantage of the second algorithm is a usage of the deterministic solution to the original stochastic problem, which can be done on any existing FEM platform (see [Hughes (2000)], for instance) with some restarting macros and the post-processing probabilistic procedures.

[2] The detailed results obtained in the transient heat transfer analysis shows quite different random response in case of uncertainty in the heat conductivity and capacity. While all probabilistic moments increase monotonously (or almost monotonously) together with time in the first case, the structure with random heat capacity exhibits

some uncontrolled growth of all those moments immediately after beginning of the transient process and further fast decay of all the studied moments. According to the adopted contrast between those parameters, the heat capacity is much more influential than the heat conductivity but it is apparent that in real engineering case study it can depend on the material being modelled (or the contrast between the constituents in composites).

[3] The stochastic generalized perturbation technique in conjunction with the modal superposition method allows for the reasonable compromise in-between computational time consumption and opportunity as well as accuracy in determination of up to the first four probabilistic moments for the structural dynamical response. According to the algorithm proposed it is possible to provide the additional analysis with a single Gaussian variable, however a change to other distribution is possible, while larger number of random input parameters, especially correlated with each other, needs some extra components adequate to the covariance matrices for both input parameters and output state variables.

[4] An application of the computer algebra systems in probabilistic and stochastic numerical studies and, especially, visualization may play a decisive role in engineering studies in this area bringing still new computational tools to speed up the traditional algorithms as well as to create the new attractive platforms for the FEM modeling with the use of traditional academic software. Further work shall focus on the nonlinear transient problems computational modelling, where the heat conductivity, capacity and the other possible sources of the uncertainty will also depend on the actual temperature distribution along the discretized system [Oden (1972)]. Although the modal superposition method is frequently advised by many engineering codes and software, other solution methods [Hughes (2000)] may also find their probabilistic realization [Lin (1961)] via the stochastic perturbation technique. On the other hand, the computer advances of this technique will allow a multivariable analyses of stochastic phenomena, where various uncertainty sources may be correlated with each other. Mathematical extension of the generalized Stochastic Finite Element Method using the RFM algorithm may be focused on inclusion of the random processes to define some physical or geometrical parameters in terms of their natural ageing or unpredictable accidents.

Acknowledgement: This paper has been financially supported by the Polish Ministry of Science and Higher Education under the grant no 519 386 636.

References

Bathe, K.J. (1996): *Finite Element Procedures*. Prentice Hall, Englewood Cliffs, New York.

Carslaw, H.S., Jaeger, J.C. (1959): *Conduction of Heat in Solids*. Oxford Univ. Press: London.

Collatz, L. (1966): *The Numerical Treatment of Differential Equations*. 3rd Edition, Springer-Verlag.

Elishakoff, I., Ren, Y.J. (1995): Some exact solutions for the bending of beams with spatially stochastic stiffness. *Int. J. Solid Struct*., vol. 32, no. 16, pp. 2315–2327.

Hien, T.D., Kleiber, M. (1997): Stochastic finite element modelling in linear transient heat transfer. *Comput. Methods Appl. Mech. Engrg*., vol. 144, pp. 111-124.

Hughes, T.J.R. (2000): *The Finite Element Method - Linear Static and Dynamic Finite Element Analysis*. Dover Publications, Inc., New York.

Hurtado, J.E. (2002): Reanalysis of linear and nonlinear structures using iterated Shanks transformation. Comput. Methods Appl. Mech. Engrg. 191:4215–4229.

Kaminski, M. (2010): An introduction to the plasticity problems using the generalized stochastic perturbation technique. *Comput. Mech*., vol. 45, no. 4, pp. 349-361.

Kaminski, M. (2011): Structural sensitivity analysis in nonlinear and transient problems using the local response function technique. *Struct. Mutlidisciplinary Optimiz*., vol. 43, no. 2, pp. 261-274.

Khuri, A.I., Cornell, J.A. (1987): Response Surfaces: Design and Analysis, Marcel Dekker, New York.

Kleiber, M. (1989): An Introduction to the Finite Element Method (in Polish). Polish Sci. Publ., Warszawa-Poznan.

Kleiber, M., Hien, T.D. (1992): *The Stochastic Finite Element Method*. Wiley, Chichester.

Krishnamoorthy, C.S. (1994): *Finite Element Analysis*. 2nd Edition, McGraw-Hill.

Lin, Y.K. (1961): *Probabilistic Theory of Structural Dynamics*, McGraw-Hill, New York.

Liu, W.K., Belytschko, T., Mani, A. (1986): Random field finite elements. *Int. J. Num. Meth. Engrg*., vol. 23, pp. 1831–1845.

Oden, J.T. (1972): *Finite Elements of Nonlinear Continua*. McGraw-Hill.

Papadopoulos, V., Papadrakakis, M., Deodatis, G. (2006): Analysis of mean and mean square response of general linear stochastic finite element systems. *Comput. Methods Appl. Mech. Engrg*., vol. 195, pp. 5454–5471.

Pepper, D.W., Heinrich, J.C. (1992): The finite element method. Series in Computational and Physical Processes in Mechanics and Thermal Sciences. Hemisphere.

Schueller, G.I. (2007): On the treatment of uncertainties in structural mechanics and analysis. *Comput. & Struct*., vol. 85, pp. 235-243.

Spanos, P.D., Tezcan, J., Tratskas, P. (2005): Stochastic processes evolutionary spectrum estimation via harmonic wavelets. *Comput. Methods Appl. Mech. Engrg*. , vol. 194, pp. 1367–1383.

Van Noortwijk, J.M., Frangopol, D.M. (2004): Two probabilistic life-cycle maintenance models for deteriorating civil infrastructures. *Prob. Engrg. Mech.*, vol. 19, pp. 345–359.